Human peripheral blood mononuclear cells targeted multidimensional switch for selective detection of bisulphite anion

Sangita Das[a*], Partha Pratim Das[b] , James W.Walton[a], Kakali Ghoshal[c], Lakshman Patra[d], Maitree Bhattacharyya[c], Tapan Kumar Mondal[d] and Sabu Thomas[e]

[a.] Durham University, Department of Chemistry. Durham, DH1 3LE, UK.

[b.] Center for Novel States of Complex Materials Research, Seoul National University, Seoul 08826, Republic of Korea

[c.] Department of Biochemistry, University of Calcutta, 35 Ballygunge Circular Road, Kolkata 700019, India.

[d.] Department of Chemistry, Jadavpur University, Jadavpur, Kolkata, India.

[e.] Mahatma Gandhi University, Kerala, India.

Abstract

A new ratiometric π-conjugated luminophore with donor-acceptor (D- π- A) network CM {(E)-2-(4-(2-(9-butyl-9H-carbazol-3-yl)vinyl)benzylidine)malononitrile} has been synthesized by malononitrile conjugated carbazole dye with an intervening p-styryl spacer. Here, p-styryl conjugated malononitrile is used as a recognition site for the detection of HSO_3^- with a fast response time (within 50 s). In a mixed aqueous solution, CM reacts with HSO_3^- to give a new product 1-(9-butyl-9H-carbazol-3-yl)-2-(4-(2, 2-dicyanovinyl)phenyl)ethane-1-sulfonic acid. The probe exhibits positive solvatofluorochromism with solid state red fluorescence. The restriction of intermolecular rotation of p-styryl conjugated malononitrile unit enhances the typical solid state fluorescence properties. The probe (CM and its corresponding aldehyde CA) also demonstrates a strong solvent dependence yielding blue to green to pink and even red fluorescence in commonly used organic solvents like n-hexane, toluene, diethyl ether (DEE),

THF, DCM, CH_3CN and MeOH. The chemodosimetric approach of HSO_3^- selectively takes place at the olefinic carbon exhibiting a prominent chromogenic as well as ratiometric fluorescence change with a 147 nm blue-shift in the fluorescence spectrum. CM can detect HSO3- as low as 1.21×10^{-8} M. Moreover, the CM can be successfully applied to detect intrinsically generated intracellular HSO_3^- in human peripheral blood mononuclear cells (PBMCs). CM has shown sharp intensities (2628 ± 511.8) when the cells are HSO_3^- untreated. At green channel (at 486 nm) almost negligible fluorescence intensities are found (423 ± 127.5) for HSO_3^- untreated samples. However, the green fluorescence (2863 ± 427.5) increases significantly ($p < 0.05$), and simultaneously the red fluorescence gets significantly ($p < 0.05$) diminished (515 ± 113.2) after addition of HSO_3^-. The CM has been effectively utilized for evaluating the bisulfite ions in food samples as well. The concentrations of HSO_3^- in diluted sugar samples have been determined with the recovery of 97.6 - 9.12%.

Key words: Fluorogenic chemosensor; Ratiometric; Detection Limit; PBMCs; Bioimaging

---

Corresponding author: Email: sangitadas2327@gmail.com and sangita.das@durham.ac.uk

1. Introduction

Reactive sulfur species (RSS) are a class of redox-active sulfur-based compounds that are formed under the conditions of oxidative stress by inhibiting thiol-proteins that play vital roles in human physiology.[1] Among the RSS, sulfur dioxide (SO_2) is the most striking compound which can act as an endogenous gasotransmitter.[2] In living organisms, especially in mammals, SO_2 is endogenously generated from the metabolism of sulfur-containing amino acid, L-cysteine catalysed by aspartate aminotransferase (AAT).[3] SO_2 plays immense physiological roles in the cardiovascular system[4] which provide a new path for cardiovascular diseases targeted therapy. Recognition of sulfur dioxide (SO_2) derivatives (bisulfite/sulfite, HSO_3^-/ SO_3^{2-}) has attracted considerable attention in the field of clinical, biological and environmental applications.[5] Superfluous consumptions of sulfur dioxide (subsequently hydrated into its derivatives to release a mixture of sulfite and bisulfite, 3:1 M/M),[6] can damage various organs (brain, lung, heart, liver and kidney). Acute and prolonged exposure of HSO_3^- might cause respiratory diseases, cardiovascular disease, lung cancer, asthma, hypotension, allergic reactions, gastrointestinal and even neurological disorders in some individuals.[7,8] On the other hand, bisulfite can be employed as an essential preservative of food (fresh fruits and vegetables), beverages and pharmaceutical products due to the exceptional bacteriostasis and antioxygenation properties of sodium bisulfite preventing the aforementioned items from oxidation and degradation.[9]

There are several methods to understand the physiological roles of SO_2 in living systems, for instance the electrochemical studies, capillary electrophoresis, flow injection analysis, chromatography and enzymatic techniques etc.[10] But, these methods incur complex pre-processing, destructive and time consuming nature and hence cannot be useful in living cells imaging directly.[11] Therefore, it is unequivocally significant to develop an effective method for

the detection of trace level of SO_2 derivatives with high sensitivity, selectivity and fast response rate. Fluorescence probes with excellent selectivity and sensitivity can be used as efficient molecular tools for sensitive detection of target analytes, bioactive molecules with in vivo imaging.[12] Albeit, few fluorescent probes have been reported for the rapid sensing of HSO_3^-, but most of them experience several limitations, such as back ground noise, long response time, poor solubility for the selectivity etc.[13] However, single fluorescent switch which can monitor highly selective and distinctive response of trace amounts of bisulfite in living systems is still scarce. Thus, it is also needful indeed to develop a specific, sensitive, highly selective probe for biological imaging of SO_2 derivative HSO_3^- anion.

On the other hand, fluorescent dyes competent to show solvent-dependent changes in their visual and fluorescent color have acclaimed importance for their solvent-polarity-sensitivity by exhibiting either negative or positive solvatochromism[14] and sensing of volatile organic compounds[15]. The typical Intramolecular Charge Transfer (ICT) dyes clearly exhibit solvatofluorochromic nature providing a sensitive response with change in micro environmental polarity[16]. Most of the solvent sensitive dyes consist of an electron rich (Donor, D) and an electron poor (Acceptor, A) moiety in a single molecule linked with a π-linker which is generally known as a D–π–A system.

Solvatochromic dyes undergo strong changes after interaction between solvent environment and fluorophore upon electronic excitation due to ICT with high dipolar excited state from a donor to acceptor moiety [17]. Therefore, tremendous amount of research studies is ongoing to develop an intramolecular charge transfer (ICT) molecule which can sense HSO_3^- and exhibit intriguing solvatochromic behavior as well. Moreover, the same efficient for bioimaging in human peripheral blood mononuclear cells (PBMCs) is extremely interesting. Considering the impact of

HSO_3^-, several research groups have reported numerous number of literature to detect HSO_3^- anion[18] but a single sensor showing brilliant solid-state red fluorescence, positive solvatofluorochromism and can detect HSO_3^- in human peripheral blood mononuclear cells (PBMCs) is extremely rare. We have also demonstrated a clear advantage of our probe in hand (CM) compared to already existing fluorescence sensors (Comparison Table S5).

In continuation to our research on synthesizing promising fluorescence sensors, [19] in this work, we have designed and synthesized a novel probe (CM) which adopted a D–π–A structure, which further makes the nucleophilic addition of HSO_3^- at the olefinic centre easier. CM manifests a selective, sensitive and fast response to HSO_3^- over other biologically and physiologically important anions and bio-thiols. More importantly, the detection has been realized by ratiometric detection mechanisms. As far as we know, this is probably the first report that shows a prominent soli-state red-light emitter along with exhibits positive solvatofluorochromic change in response to HSO_3^- and can operate in PBMCs for bioimaging.

2. Experimental

2.1. Material and methods

All materials Chemicals and solvents were purchased from Sigma-Aldrich Chemicals Private Limited and were used without further purification. For column chromatography silica gel (100-200 mesh, Merck) was used. ^{1}H NMR and ^{13}C NMR spectra were recorded on a Varian VXR-400 spectrometer instrument (^{1}H at 399.97 Hz, ^{13}C at 125.75 MHz) commercially available $CDCl_3$, with tetramethylsilane (TMS) as an internal standard. In NMR spectroscopy, the chemical shifts are expressed in δ units and coupling constants in Hz. UV-Vis titration spectra were recorded on Cary 5000 high performance UV-Vis-NIR spectrophotometer, controlled by Cary WinUV software spectrophotometer. Fluorescence experiments was recorded using a

Horiba Fluorolog-3 spectrometer using FluorEssence software with a fluorescence cell of 10 mm path quartz cuvette. For the UV-Vis and fluorescence titration experiment we used the anions viz. [Hcy, S^{2-}, F^{-}, Cl^{-}, HSO_4^{-}, HSO_3^{-}, SO_4^{2-}, NO_3^{-}, CN^{-}, AcO^{-}, PPi, and Pi] as their sodium salts and cations as their chloride salts (Na^{+} and K^{+})

2.2. General method of UV-Vis absorption and fluorescence emission titrations:

For both UV-Vis and fluorescence titrations, a stock solution of CM was prepared (20 μM) in CH_3OH-H_2O (1:4, v/v) in the presence of HEPES buffer (10 mM) solution at pH = 7.2. The solution of the guest anions using their sodium salts at 20 μM were prepared in buffered deionized water at pH 7.2. The solution of the sensor was prepared by an appropriate dilution technique.

2.2. Synthesis

2.2.1. Synthesis of compound CM {(E)-2-(4-(2-(9-butyl-9H-carbazol-3-yl)vinyl)benzylidine)malononitrile}:

The final compound (CM) were prepared following the synthetic route depicted in the scheme 1. The synthesis up to the compound CA (5) was previously reporter by us.[20] A mixture of CA (353 mg, 1.00 mmol) and Malononitrile (66 mg, 1.00 mmol) was heated in refluxing condition for 6 h in anhydrous acetonitrile solution (20 ml). After 6 h, the reaction mixture was cooled and the solvent was then removed under reduced pressure to give a reddish brown solid residue. This residue was further purified by column chromatography (silica gel, 15% ethyl acetate in petroleum ether) to give the probe CM as a crystalline red solid (530 mg, 74%).

^{1}H NMR (500 MHz, $CDCl_3$): δ 0.96 (t, *J* = 7.25 Hz, 3H), 1.41 (sextet, *J* = 7.5 Hz, 2H), 1.86 (m, 2H), 4.31 (t, *J* = 7.25 Hz, 2H), 7.14 (m, 1H), 7.27 (m, 1H), 7.45 (m, 4H), 7.66 (m, 4H), 7.88 (d, *J* = 8.5 Hz, 2H), 8.12 (d, *J* = 8 Hz, 1H), 8.25 (s, 1H).

^{13}C NMR (125 MHz, $CDCl_3$): δ 13.99, 20.68, 31.25, 43.18, 80.36, 109.25, 113.32, 114.44, 119.55, 119.80, 120.61, 122.91, 123.52, 124.05, 125.07, 126.30, 126.65, 127.01, 127.50, 129.41, 131.66, 134.81, 141.12, 144.93, 158.89.

HRMS (ESI, positive): Calcd. for $C_{28}H_{23}N_3$ $[M]^+$ (m/z): 401.1892; found: 401.1880.

Melting Point: > 300 ^{o} C (decomposed).

2.2.2. HSO_3^- complex of CM

For the synthesis of the HSO_3^- complex of CM, the probe, CM (50 mg, 0.12 mmol) and $NaHSO_3$ (15 mg, 0.14 mmol) were dissolved in methanol (10 ml) and the mixture was refluxed for 4 hours. The yellow coloured reaction mixture solution was cooled and a yellow precipitate collected by filtration and dried in vacuum. The solid product (CM-HSO_3) was used for ^{1}H NMR and ESI-MS spectroscopy.

^{1}H NMR (400 MHz, $CDCl_3$): δ 0.97 (t, *J* = 7.6 Hz, 3H), 1.36 (q, *J* = 8 Hz, 2H), 1.88 (m, 2H), 4.21 (t, *J* = 6 Hz, 2H), 5.05 (m, 1H), 6.87 (d, *J* = 8 Hz, 2H), 7.02 (m, 4H), 7.18 (m, 4H), 7.40 (t, *J* = 8 Hz, 2H), 7.55 (t, *J* = 8 Hz, 1H), 7.81 (d, *J* = 7.2 Hz, 1H), 9.82 (s, 1H).

HRMS (ESI, Positive mode): calcd. for $C_{28}H_{27}N_3NaO_4S$ [CM-HSO_3 + Na^+ + H_2O]+ (m/z): 524.1614; found: 524.1684.

3. Results and discussion

3.1. Synthesis of the probe CM

The desired probe CM is synthesized as shown in Scheme 1. All the structures from 1-5 have prepared according to the procedures reported elsewhere.[20] Refluxing condensation of CA with malononitrile for 6 hours yields the probe (CM) as red solid. The probe is characterized by ^{1}H NMR, ^{13}C NMR and HRMS (Fig. S9-S11, ESI). CA and CM exhibit yellow and red

fluorescence in the solid state, respectively, owing to the intriguing AIE effect and packing arrangements. All the probes show solvatofluorochromism originated from the ICT character.

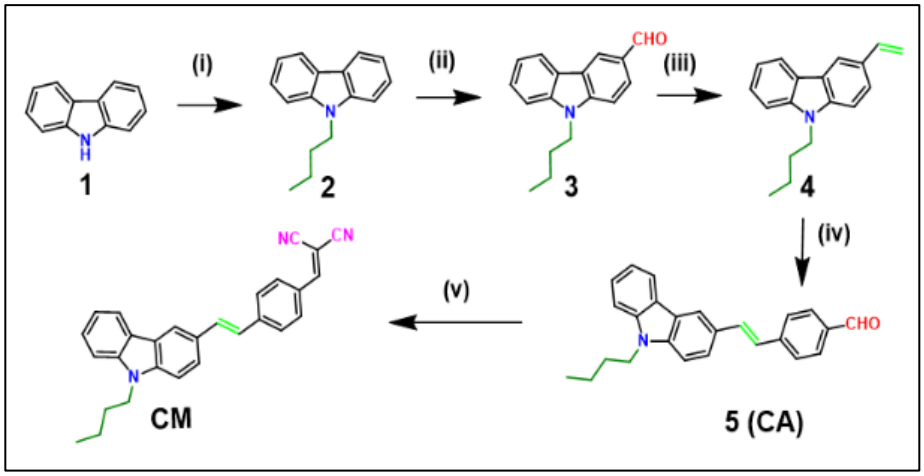

Scheme 1: Synthesis of the receptor (CM). Reagents and conditions: (i) n-Butyl bromide, 30% aqueous NaOH solution, DMSO, 70-80 °C, 16 h, 95%; (ii) DMF/$POCl_3$, 50-60 °C, 12 h, 87%; (iii) methyltriphenylphosphonium bromide, ^{t}BuOK, THF, 0 °C to rt, 12 h, 72%; (iv) p-bromobenzaldehyde, $Pd(OAc)_2$, KOAc, PPh_3, DMF, 80-90 °C, 12 h, 80%; (v) Malononitrile, acetonitrile, Reflux, 6h.

3.2. Solvatofluorochromism study:

Both the final probes CM and the corresponding aldehyde CA consist of the D-π-A electronic structural arrangement showing positive solvatofluorochromism, which mainly appeared from the Internal Charge Transfer (ICT) mechanism. In order to establish this organic solvent-sensitive characteristic, the absorption (Fig. S4, ESI) and fluorescence emission properties of CM and CA have been carried out which reveal positive solvatofluorochromism. The emission maximum shows red shift in different organic solvents with varying polarity from lower to higher where CM has been investigated in n-hexane, toluene, diethyl ether (DEE), THF, DCM,

CH_3CN and MeOH and CA in n-hexane, toluene, THF, DCM, CH_3CN, DMSO and MeOH (Fig. 1). For instance, the emission maximum of CM and CA appearing at 524 and 437 nm, respectively, in the least polar n-hexane, whereas those peaks at 677 and 593 nm, respectively, in MeOH, the most polar solvent in this study evidence that the ICT based probes are highly sensitive to solvent polarity (Fig. 1).

Moreover, a distinct solvent dependent change in the fluorescence color is observed for them. CM depicts a prominent color change from green→ pink→ red, while the course of color shifts from blue→ cyan→ green→ orange for CA with increasing the solvent polarity. The significant red shift of the emission maximum of CM (Δf = 153 nm) and CA (Δf = 156 nm) can be attributed to the higher polar nature of the carbazole-based chromophores which produce extra stabilization in the excited-state compared to the ground electronic state in polar solvents. This also suggests the higher polarization of the excited states of both the probes compared to the ground states.[21] Therefore, the two probes can be successfully employed as a sensitive solvent polarity sensor and the data are provided in Table S1 and S2 (ESI).

3.3. Solid State Fluorescence Study:

Electron-rich carbazole conjugated fluorophores are also substantiated as efficient electron transport materials owing to their molecular geometries and packing arrangements. The compactness of the carbazole-conjugated systems is well organized based on intermolecular interactions. The incorporation of the p-styryl conjugated spacer in the carbazole system further restricts the intramolecular vibration and rotational freedom which may lead the probe to exhibit prominent fluorescence in the solid state. In particular, the intense red and green fluorescence of CM and CA under hand held ultraviolet irradiation confirms their emissive characteristic in solid

state (Fig. 3; inset). The strong emission of CM and CA maximizes, respectively, at 625 and 505 nm upon excitation at 480 and 390 nm as displayed in Fig. 3.

3.2. Sensing property of the probe CM in solution:

3.2.1. UV-Vis Study:

The initial spectroscopic characteristics have been investigated by monitoring the UV-Vis absorption study of the probe CM in a mixed aqueous methanol medium. After a number of measurements, a strong absorbance maximum at 433 nm repeatedly observed for the probe in absence of any guest analytes indicates that the probe in hand is well stable under these physiological conditions. The addition of trace amounts of HSO_3^- causes a prominent change in the UV-Vis profile. The absorption band at 433 nm is found to decrease gradually with simultaneous increase in the band at 341 nm. An optimized aqueous solution (H_2O/MeOH, 4/1, v/v, 10 mM PBS, pH = 7.3) has been prepared thereafter for better understanding the mechanism and establishing the probe more suitably for environmental and biological applications. Here, the selectivity study of the probe has been tested by employing different guest analytes, namely, Homocystein (Hcy), S^{2-}, F^-, Cl^-, HSO_4^-, HSO_3^-, SO_4^{2-}, NO_3^-, CN^-, AcO^-, PPi, and Pi. It is worth observing that the probe performs promptly only after addition of HSO_3^-, whereas the other aforementioned analytes remain inactive in exhibiting any significant change in the UV-Vis spectra (Figure 4a and b). A rapid decrement in the peak at 433 and a notable development of the peak in the UV region at 341 nm through a well-defined isosbestic point at 357 nm are observed in this regard after gradual addition of HSO_3^- (0- 5 equiv.) (Fig. 4a). The change in absorbance profile after addition of HSO_3^- may be attributed to the chemodosimetric approach of HSO_3^- to the olefinic carbon which rearranges to give the reaction based product 1-(9-butyl-9H-carbazol-

3-yl)-2-(4-(2,2-dicyanovinyl)phenyl)ethane-1-sulfonic acid. The ratio of the absorbance intensity of the two peak (A_{341}/A_{433}) is plotted with varying the concentration of HSO_3^- which shows a good linear relationship in the range of 0-11.6 μM (R^2= 0.99, Fig. S2, Fig. S3a, ESI).

3.2.2. Fluorescence study:

We have also monitored the spectral behavior of CM based on the fluorescence study with different analytes. In this analysis, the emission characteristics of the probe is carried out in a mixed aqueous methanol system (10 μM, H_2O/MeOH, 4/1, v/v, 10 mM PBS, pH = 7.3) at room temperature. The probe in hand exhibits a strong emission peak with a maximum at 633 nm upon excitation at 410 nm. The fluorescence spectral changes have been investigated by adding HSO_3^- and several guest analytes in a mixed aqueous solution at room temperature.

The peak at 633 nm is found to decrease gradually and simultaneously a new peak at 486 nm appears with an isoemissive point at about 562 nm after interaction with HSO_3^- (Fig. 5a). The isosbestic point and the isoemissive point were seemed to be slightly shifted which may be attributed to the small change of pH during the titration. To establish the chemodosimetric mechanism in a more explicit way, we have studied the reaction between the probe in hand and HSO_3^- by mass spectra. The prominent peak (100 %) in the ESI-MS spectrum at m/z 524.1684 can be assigned to the CM-SO_3H adduct $[M+Na+H_2O]^+$ formed in-situ (Fig. S12, ESI). The observed enhancement in the emission intensity at 486 nm upon addition of HSO_3^- is therefore related to the chemodosimetric attack of HSO_3^- at the olefin carbon of CM. Thus, the in-situ formation of CM-SO_3H adduct leads to the 'ICT-off' mechanism which is proposed later in Scheme 2.

The selectivity in fluorogenic response of CM has also been verified by using different guest analytes, namely Hcy, S^{2-}, F^-, Cl^-, HSO_4^-, SO_4^{2-}, NO_3^-, CN^-, AcO^-, PPi, and Pi even in excess

amount. Almost all the guest analytes, especially Hcy, SO_4^{2-} are unable to make any significant change in the emission spectrum of the receptor (Fig 5b). Only HSO_3^- is successful in bringing about prominent ratiometric change including a large blue shift ~ 147 nm of the fluorescence profile. This experiment indicates that this probe is exclusive in detecting HSO_3^- in presence of other important guest analytes. The emission intensity ratio of the two peak of CM (I_{486}/I_{633}) with varying HSO_3^- concentration again offers a good linear relationship with R^2 value 0.99 (Fig. S1, ESI). From the plot the detection limit of HSO_3^- derived is 1.21×10^{-8} M using the equation DL = K × Sb1/S where K is considered as 3 and Sb1 and S defines the standard deviation of the blank solution and the slope of the calibration curve, respectively (Fig. S1, ESI) [22]. This clears that the probe CM is highly efficient in detecting HSO_3^-. Moreover, the calculated 0.44, respectively, where rhodamine-B (φ =0.66 in ethanol) has been used as reference (ESI).

3.2.3. Selectivity and sensitivity study:

Selectivity and sensitivity are the two most crucial parameters which evaluate the ability of any sensory device. The selectivity of the probe in hand (CM) is assessed based on the fluorescence titration study. As far as the specificity of the probe towards HSO_3^- is concerned, the emission intensity of the CM solution at 486 nm has been measured in presence of 2.0 equiv. HSO_3^- where the aforementioned guest analytes are also added successively in a quite excess concentration ~ 3.0 equiv. The findings of these typical experiments as exhibited in Fig. 6 reveal that the efficiency of detection of HSO_3^- by CM remains almost unaffected in presence of other interfering guest analytes even in excess amount.

3.3. Potetnial binding mechanism:

The sensing mechanism for the recognition of HSO_3^- by CM is demonstrated in Scheme 2. The chemodosimetric addition product (CM-HSO_3) between CM and HSO_3^- is established and

confirmed by the ^{1}H NMR titration experiment. The photophysical color change of CM signifies the chemodosimetric conjugate addition reaction of HSO_3^- at the olefinic carbon of the p-styryl moiety, which further hampers the π-conjugation and consequently all of the ^{1}H NMR signals undergo an up-field shift. In particular, the significant up-field shift of the vinyl protons from δ 8.25 and 8.12 to δ 4.95 and 5.04 strongly evidences the chemodosimetric approach of HSO_3^- at the ethylene group (Fig. S13, ESI).

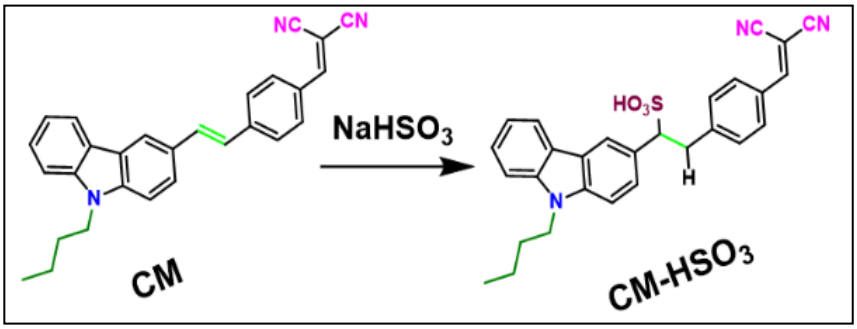

Scheme 2. Plausible mechanism for the recognition of HSO_3^- by CM.

3.4. pH Study:

We have also verified the influence of pH on the fluorescence response of CM in presence of HSO_3^-. Firstly, no significant change in the fluorescence emission of CM was studied from pH 3.0-12 defines the stability of the probe itself throughout a wide pH range which suggest its potential for applying in biological samples. The fluorescence of CM has been recorded further after the treatment with HSO_3^-. Interestingly, the emission of the CM–HSO_3 system remains almost invariant in the acidic pH, but the characteristic emission peak related to HSO_3^- detection at 486 nm is found to get considerably influenced at the basic pH beyond 7.6 (Fig. S5, ESI). Thus, it becomes clear that the CM can be employed as an efficient fluorescence tool to recognize the HSO_3^- in biological samples at near neutral pH.

3.5. Cell viability and bioimaging studies:

The cell viability and bioimaging studies are also performed. Cell viability is represented in Figure 7, where up to 50 μM concentrations of CM shows around 55.36% (without HSO_3^-) & 52.71% (with 10 μM HSO_3^-) of viable cells respectively predicting it is a safe probe to use in a biological system. We have used 10 μM CM solutions for imaging which shows high number of viable cells (84.11% without HSO_3^- and 80.38% with HSO_3^-) concluding its nontoxic nature. The size chart for the cells is also given (20 micrometer). In Fig. 8, we can see that at red channel (at 633 nm), CM has shown sharp intensities (2259.3 ± 124.1) when the cells were HSO_3^- untreated. At green channel (at 486nm) almost negligible fluorescence intensities are found (533.6 ± 25.2) for HSO_3^- untreated samples. However, when HSO_3^- has been added significant increase ($P < 0.05$) in green fluorescence (2295 ± 124.8) was observed. The red fluorescence got significantly ($P < 0.05$) diminished (537 ± 29.8) after addition of HSO_3^-. The P values were calculated using one-way ANOVA followed by multiple comparison for differences between groups. All the statistical analysis were carried out using GraphPad Prism 8 software. We have replicated this experiment 6 times following identical conditions and provided more bio-imaging data in the supplemental document. We have provided bright field images along with the fluorescence images for each experiment. CM has good cell permeability as well as stability at biological pH (7.4). Our MTT (3-(4, 5-dimethylthiazolyl-2)-2, 5-diphenyltetrazolium bromide) assay) data indicates its safe and non-toxic nature towards cell. It does not cause cell damages such as swelling or lysis. CM is highly sensitive towards HSO_3^- and a dose as low as 25 μM can be easily detected by fluorescence microscopy. Therefore, this fluorescence probe is safe to use for biological samples to detect HSO_3^- endogenously.

3.6. Reaction kinetic Study:

The study of the reaction kinetics (response rate) is surely an important requirement for any chemodosimeter. That has been done here by measuring the fluorescence spectra of CM adding 2 equivalents of HSO_3^-. The variation in the fluorescence emission intensity at 486 nm is plotted with the time course of the reaction with HSO_3^- (ESI, Fig. S8). It is important to observe that they are following a linear relationship up to only ~50 seconds while the entire experiment has been carried out up to 2 minutes. This ensures the completion of the chemodosimetric reaction between CM and HSO_3^- before 60 seconds which highlights that CM can be effectively used as a real-time monitoring kit for HSO_3^-. However, based on the first order rate equation a reasonable rate constant 5.72×10^{2} Sec^{-1} is derived from the aforementioned plot in the present study.

3.7. Excited state behaviour Study:

The excited state behaviour of the probe CM and it's adduct with HSO_3^- is examined by the nanosecond time-resolved fluorescence technique (Fig. 9). Probe has a comparably low lifetime value, t = 1.7 ns ($\varkappa^2$ = 1.21), after formation of the adduct with HSO_3^- the excited state lifetime increases remarkably, t = 9.32 ns ($\varkappa^2$ = 1.1). Radiative rate constant kr and total non-radiative rate constant $k$nr have been calculated using the equation[23] $\tau^{-1} = k\text{r} + k\text{nr}$ for both the CM and CM-SO_3H species (Table S3, ESI). The change in the value of τ, kr and $k$nr indicates the adduct formation of HSO_3^- with the probe CM to form a new fluorogenic compound CM-SO_3H which have higher lifetime than the probe itself.

3.8. Dip-Stick Study:

In order to apply as Test-Kit, the TLC plates are prepared and immersed in the solution of CM (0.10 mM, in CH_3CN). After drying in air, the same plate has been dipped in a solution of HSO_3^- (0.10 mM, in CH_3CN). Interestingly, the TLC plate changes its color very fast within 10 Sec. The distinct color change of the TLC plates under ambient light and hand-held UV light can be

perceived from the photos displayed in Fig. 10. This simple 'Dip-Stick' technique establishes the particular probe as a highly sensitive candidate for the qualitative and instant detection of HSO_3^- visible to the naked eye and therefore can be utilized as a portable kit for sensing HSO_3^-.

3.9. Food Sample Analysis:

Bisulfite is widely used as the preservative for food products. But, consumption of excess bisulfite can lead to adverse health hazards.[24] Considering the high sensitivity of CM towards HSO_3^-, we have further explored the probe for the detection of the trace amount of HSO_3^- in real food sample. In a typical experiment 5 g of sugar has been dissolved and diluted in 50 ml water. After that, 5 μM CM has been added to the sugar solution spiked with the bisulfite of various concentration. Based on the fluorescence titration the concentrations of HSO_3^- have been determined with excellent recovery of 97.6 to 99.12% as mentioned in Table S4. The high accuracy of the probe strongly supports its potential to be employed as a promising candidate to quantify the bisulfite in food samples as well.

4. Conclusion

In summary, we have demonstrated a new fluorescence switch (CM) which is successfully designed and synthesized by the perfect blending of malononitrile conjugated carbazole dye with an intervening p-styryl spacer. This D-π-A carbazole-based dye CM and its corresponding aldehyde CA respectively exhibit a prominent red and green solid-state fluorescence. The probe shows intriguing solvatofluorochromism originated from the donor-acceptor arrangement contributing a significant intramolecular charge transfer. The probe is found to be highly potential in detecting HSO_3^- based on the ICT chemodosimetric mechanism. The absorption and emission experiments manifest the ratiometric sensing of HSO_3^- with a low detection limit 1.21×10^{-8} M. The specific response of the probe towards HSO_3^- is attributed to the nucleophilic

conjugate addition between the electron-deficient C=C and HSO_3^- which is established by the ^{1}H-NMR and ESI-mass spectra. As far as the biological utilizations are concerned, the probe is found to be extremely safe and effectively recognizing HSO_3^- in human peripheral blood mononuclear cells as well as in real food samples. The 'Dip-Stick' study also refers to the probe to be used as a portable kit for the instant detection of HSO_3^-. This new probe, which has excellent selectivity and cellular application has the potential to be very important for non-invasive detection of the important analyte HSO_3^-.

5. Conflicts of interest

There are no conflicts to declare.

6. Acknowledgment

S. Das Acknowledges Newton International Fellowships Royal Society (UK) for fellowship (ref: NIF\R1\182209). S. Das Acknowledges Dr. Krishnendu Aich, Department of Chemistry, Jadavpur University for helping in the excited state behaviour study of the compound.

7. Reference

[1] X. Y. Jiao, Y. Li, J. Y. Niu, X. L. Xie, X. Wang, B. Tang, Small-Molecule Fluorescent Probes for Imaging and Detection of Reactive Oxygen, Nitrogen, and Sulfur Species in Biological Systems, Anal. Chem., 90 (2018) 533.

[2] (a) Y. Zhao, H.A. Henthorn, M.D. Pluth, Kinetic Insights into Hydrogen Sulfide Delivery from Caged-Carbonyl Sulfide Isomeric Donor Platforms, J. Am. Chem. Soc. 139 (2017) 16365; (b) Z. B. Du, B. Song, W. Z. Zhang, C. C. Duan, Y. L. Wang, C. L. Liu, R. Zhang, J. L. Yuan, Quantitative Monitoring and Visualization of Hydrogen Sulfide In Vivo Using a Luminescent Probe Based on a Ruthenium (II) Complex, Angew. Chem. Int. Ed. 57 (2018) 3999; (c) K. A. Pardeshi, G. Ravikumar, H. Chakrapani, Esterase Sensitive Self-Immolative Sulfur Dioxide Donors, Org. Lett. 20 (2018) 4.

[3] P. Bora, P. Chauhan, K. A. Pardeshi. H. Chakrapani, Small molecule generators of biologically reactive sulfur species, RSC Adv. 8 (2018) 27359.

[4] Z. Xu, L. Xu, Fluorescent probes for the selective detection of chemical species inside mitochondria, Chem. Commun. 52 (2016) 1094.

[5] (a) C. Suksai, T. Tuntulani, Chromogenic anion sensors, Chem. Soc. Rev. 32 (2003) 192; (b) P. Molina, F. Zapata, A. Caballero, Anion Recognition Strategies Based on Combined Noncovalent Interactions, Chem. Rev. 117 (2017) 9907.

[6] (a) Y. Liu, K. Li, M. Y. Wu, Y. H. Liu, Y. M. Xie, X. Q .Yu, A mitochondria-targeted colorimetric and ratiometric fluorescent probe for biological SO_2 derivatives in living cells, Chem. Commun. 51 (2015) 10236; (b) W. Xu, C. L. Teoh, J. Peng, D. Su, L. Yuan, Y. T. Chang, A mitochondria-targeted ratiometric fluorescent probe to monitor endogenously generated sulfur dioxide derivatives in living cells. Biomaterials. 56 (2015) 1; (c) J. Song, D. Zhang, Y. Liu, Y. Zhao, Y. Ye, A highly sensitive and selective turn-on fluorescent probe for sulfite and its application in biological imaging, New J. Chem. 39 (2015) 6284.

[7] (a) S. Iwasawa, Y. Kikuchi, Y. Nishiwaki, M. Nakano, T. Michikawa, T. Tsuboi, S. Tanaka, T. Uemura, A. Ishigami, H. Nakashima, T. Takebayashi, M. Adachi, A. Morikawa, K. Maruyama, S. Kudo, I. Uchiyama, K. Omae, Effects of SO_2 on Respiratory System of Adult Miyakejima Resident 2 Years after Returning to the Island, J. Occup. Health, 51 (2009), 38; (b) N. Duan, S. Yang, H. Tian, B. Sun, The recent advance of organic fluorescent probe rapid detection for common substances in beverages, Food Chemistry, 358 (2021) 129839;

[8] (a) N. Sang, Y. Yun, H. Li, L. Hou, M. Han, G. Li, SO_2 Inhalation Contributes to the Development and Progression of Ischemic Stroke in the Brain, Toxicol. Sci. 114 (2010) 226; (b) K. Li, L.-Ling Li, Q. Zhou, K.-K. Yu, J. S. Kim, X.-Q. Yu, Reaction-based fluorescent probes for SO_2 derivatives and their biological applications, Coord. Chem. Rev. 388 (2019) 310;

[9] (a) Y. Sun, S. Fan, S. Zhang, D. Zhao, L. Duan, R. Li, A fluorescent turn-on probe based on benzo[*e*]indolium for bisulfite through 1, 4-addition reaction, Sens. Actuators, B. 193 (2014) 173; (b) G. Xu, H. Wu, X. Liu, R. Feng, Z. Liu, A simple pyrene-pyridinium-based fluorescent probe for colorimetric and ratiometric sensing of sulfite, Dyes Pigm. 120 (2015) 322; (c) S.-H. Park, N. Kwon, J.-H. Lee, J. Yoon, I. Shin, Synthetic ratiometric fluorescent probes for detection of ions, Chem. Soc. Rev., 49 (2020) 143.

[10] (a) T. J. Dale, J . Rebek, Fluorescent Sensors for Organophosphorus Nerve Agent Mimics, J. Am. Chem. Soc. 128 (2006) 4500; (b) B. Li, M. J. Chen, L. Guo, Y. Yun, G. K. Li, N. Sang, Endogenous 2-Arachidonoylglycerol Alleviates Cyclooxygenases-2 Elevation-Mediated Neuronal Injury From SO_2 Inhalation via PPARγ Pathway, Toxicol. Sci. 147 (2015) 535.

[11] (a) D. Jiménez, R. Martínez-Máñez, F. Sancenón, J. V. Ros-Lis, A. Benito, J. Soto, A New Chromo-chemodosimeter Selective for Sulfide Anion, J. Am. Chem. Soc. 125 (2003) 9000; (b) A. N. de Macedo, M. I. Y. Jiwa, J. Macri, V. Belostotsky, S. Hill, P. Britz-McKibbin, Strong Anion Determination in Biological Fluids by Capillary Electrophoresis for Clinical Diagnostics, Anal. Chem. 85 (2013**)** 11112.

[12] J. X. Ong, C. S. Q. Lim, H. V. Le, W. H. Ang, A Ratiometric Fluorescent Probe for Cisplatin: Investigating the Intracellular Reduction of Platinum (IV) Prodrug Complexes, Angew. Chem. 58 (2019) 164.

[13] L. Zhu, J. Xu, Z. Sun, B. Fu, C. Qin, L. Zeng, X. Lu, A twisted intramolecular charge transfer probe for rapid and specific detection of trace biological SO_2 derivatives and bio-imaging applications, Chem. Commun. 51 (2015) 1154.

[14] P. Cheng, J. Zhang, J. Huang, Q. Miao, C. Xu, K. Pu, Near-infrared fluorescence probes to detect reactive oxygen species for keloid diagnosis, Chem. Sci. 9 (2018) 6340.

[15] J. M. Rankin, Q. Zhang, M. K. LaGasse, Y. Zhang, J. R. Askim, K. S. Suslick, Solvatochromic sensor array for the identification of common organic solvents, *Analyst*, 140 (2015) 2613–2617.

[16] S. M. Usama, T. Thompson, K. Burgess, Productive Manipulation of Cyanine Dye π-Networks, *Angew. Chem. Int. Ed.* 58 (2019) 8974.

[17] (a) J. O. Hernández, J. Portilla, Synthesis of Dicyanovinyl-Substituted 1-(2-Pyridyl) pyrazoles: Design of a Fluorescent Chemosensor for Selective Recognition of Cyanide, *J. Org. Chem*. 82 (2017) 13376; (b) H. A. Shindy, Structure and solvent effects on the electronic transitions of some novel furo / pyrazole cyanine dyes, *Dye. Pigment.* 149 (2018) 783.

[18] (a) M. M. Fortibui, D. W. Yoon, J. Y. Lim, S. Lee, M. Choi, J. S. Heo, J. Kim, J. Kim, A cancer cell-specific benzoxadiazole-based fluorescent probe for hydrogen sulfide detection in mitochondria, *Dalton Trans*. 50 (2021) 2545; (b) Q. Liu, Y. Zhao, Y. Zhang, K. Xie, R. Liu, B. Ren, Y. Yan, L. Li, A spiropyran functionalized fluorescent probe for mitochondria targeting and imaging of endogenous hydrogen sulfide in living cells, Analyst. 145 (2020) 8016; (c) S. Li, D. Cao, Z. Hu, Z. Li, X. Meng, X. Han, W. Ma, A chemosensor with a paddle structure based on a BODIPY chromophore for sequential recognition of Cu^{2+} and HSO_3^-, RSC Adv. 9 (2019) 34652; (d) S. Roy, A. Maity, N. Mudi, M. Shyamal, A. Misra, Rhodamine scaffolds as real time chemosensors for selective detection of bisulfite in aqueous medium, *Photochem. Photobiol. Sci*. 18 (2019) 1342; (e) K. R. Everitt, H. C. Schmitz, A. Macke, J. Shan, E. Jang, B. E. Luedtke, K. A. Carlson, H. Cao, Investigation of a Sensing Strategy Based on a Nucleophilic Addition Reaction for Quantitative Detection of Bisulfite (HSO_3^-), *J. Fluorescence*, 30 (2020) 977; (f) F. Li, L. Zou, J. Xu, F. Liu, X. Zhang, H. Li, G.

Zhang, X. Duan, A high-performance colorimetric fluorescence sensor based on Michael addition reaction to detect HSO_3^- in real samples, Journal of Photochemistry & Photobiology, A: Chemistry. 411 (2021) 113201.

[19] (a) S. Goswami, S. Das, K. Aich, B. Pakhira, S. Panja, S. Mukherjee, S. Sarkar, A Chemodosimeter for the Ratiometric Detection of Hydrazine Based on Return of ESIPT and Its Application in Live-Cell Imaging, Org. Lett. 15 (2013) 5412; (b) S. Goswami, K. Aich, S. Das, A. K. Das, D. Sarkar, S. Panja, T. K. Mondal, S. Mukhopadhyay, A red fluorescence 'off–on' molecular switch for selective detection of Al^{3+}, Fe^{3+} and Cr^{3+}: experimental and theoretical studies along with living cell imaging, Chem. Commun. 49 (2013) 10739; (c) S. Goswami, S. Das, K. Aich, D. Sarkar, T. K. Mondal, C. K. Quah, H. K. Fun, CHEF induced highly selective and sensitive turn-on fluorogenic and colorimetric sensor for Fe^{3+}, *Dalton Trans*. 42 (2013)15113.

[20] K. Aich, S. Das, S. Goswami, C. K. Quah, D. Sarkar, T. K. Mondal, H. K. Fun, Carbazole benzimidazole based dyes for acid responsive ratiometric emissive switches, New J.Chem. 40 (2016) 6907.

[21] V. G. Machado, R. I. Stock, C. Reichardt, Pyridinium N-Phenolate Betaine Dyes, Chem. Rev. 114 (2014) 10429.

[22] (a) M. Shortreed, R. Kopelman, M. Kuhn, B. Hoyland, Fluorescent fiber-optic calcium sensor for physiological measurements, Anal. Chem. 68 (1996) 1414; (b) W. Lin, L. Yuan, Z. Cao, Y. Feng, L. Long, A Sensitive and Selective Fluorescent Thiol Probe in Water Based on the Conjugate 1, 4-Addition of Thiols to α,β-Unsaturated Ketones, Chem. – Eur. J. 15 (2009) 5096.

[23] Valeur, Molecular Fluorescence. Principles and Applications; Wiley-VCH: Weinheim, Germany; **2002**.

[24] Vally H, LA Misso N, Gastroenterol Hepatol Bed Bench., **2012** Winter; *5*(1): 16–23.

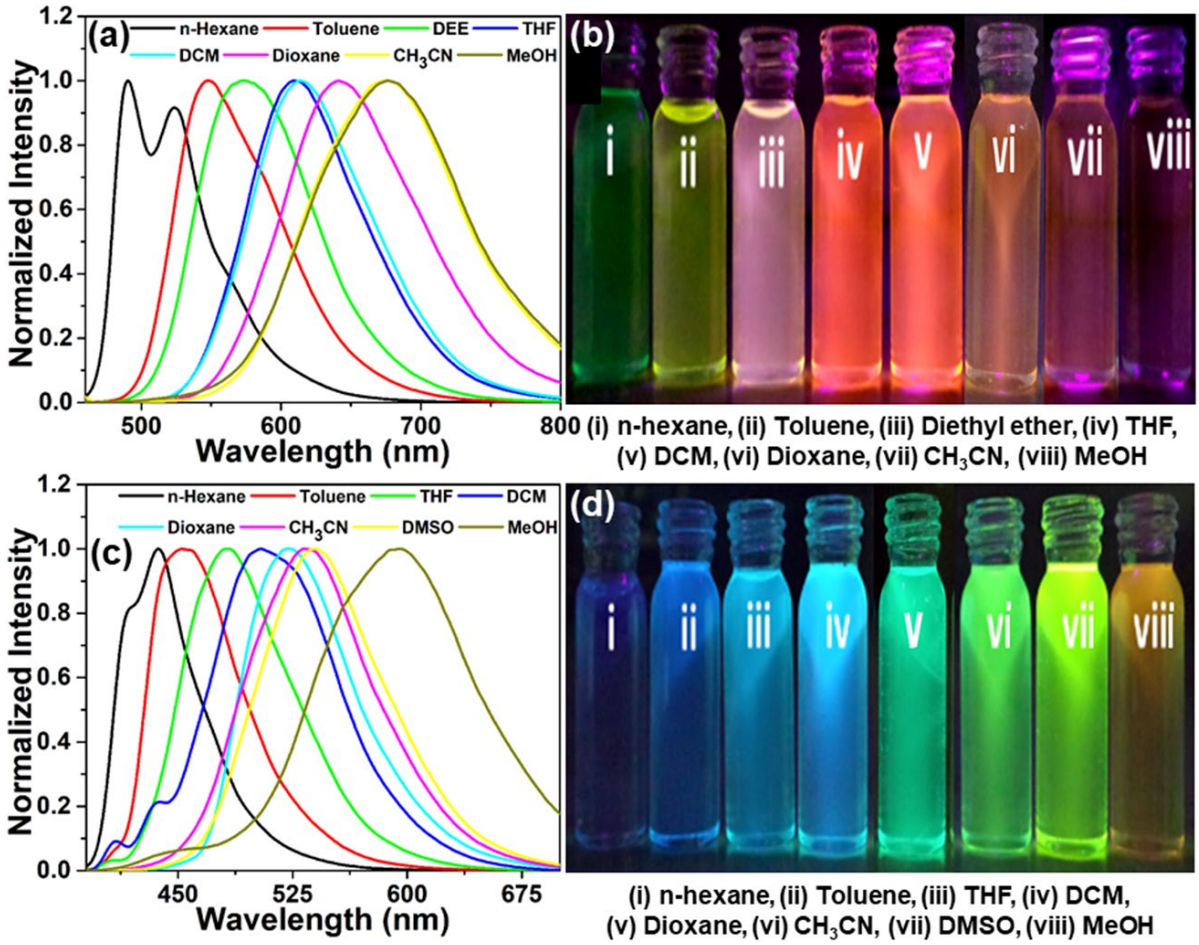

Fig 1: (a) & (c) Solvent-dependent emission spectra of CM and CA (5 μM, λ_{ex} = 450 nm and 380 nm respectively); (b) Photos of CM solution (5 μM) in different solvent under UV light (from left to right: n-hexane, toluene, diethyl ether (DEE), THF, DCM, Dioxane, CH_3CN and MeOH), (d) Photos of CA solution (5 μM) in different solvent under UV light (from left to right: n-hexane, toluene, THF, DCM, CH_3CN, DMSO and MeOH).

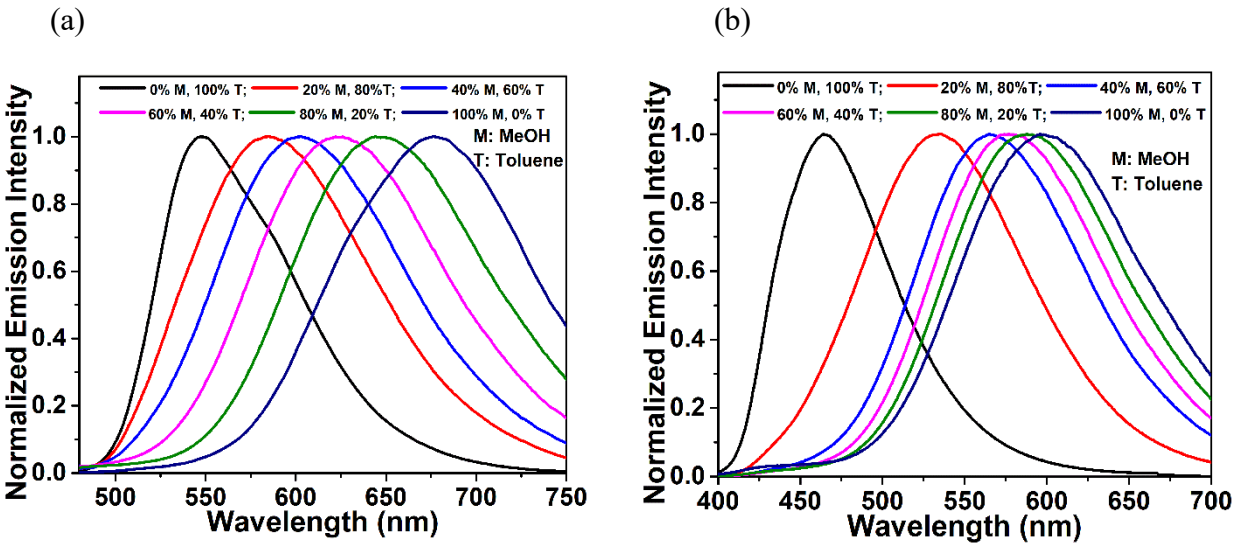

Fig 2: The fluorescence spectra of (a) CM and (b) CA in varying concentrations of Toluene in MeOH.

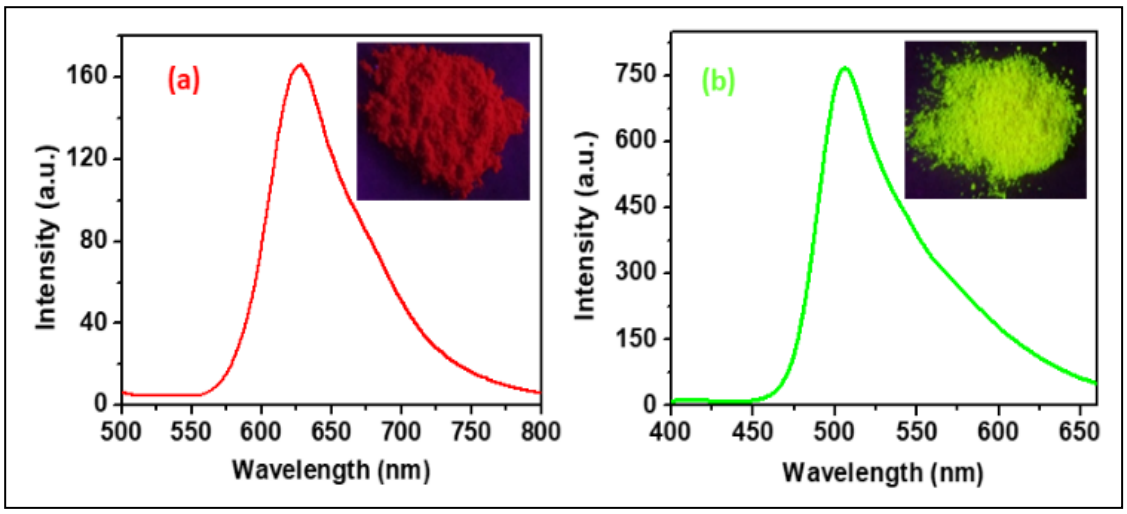

Fig 3: Fluorescence spectra of (a) CM and (b) CA in solid state

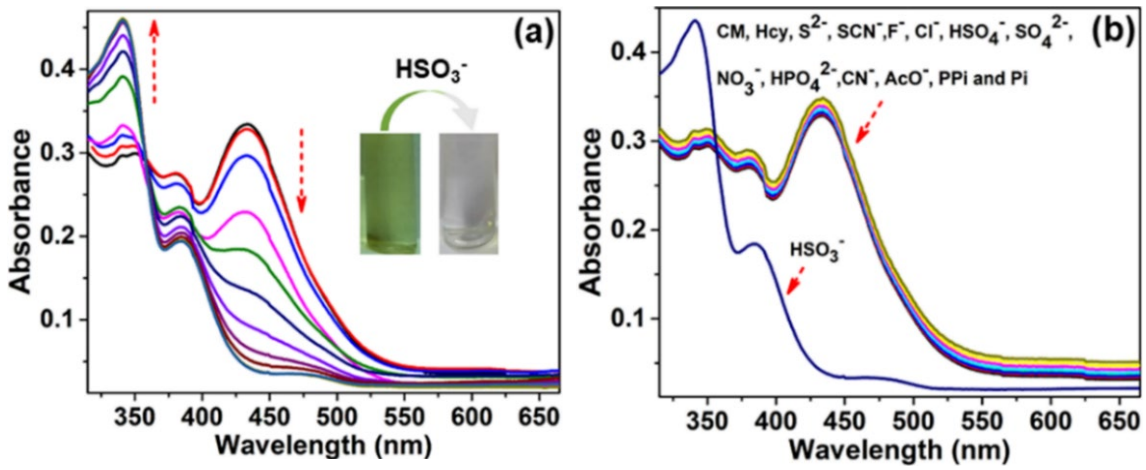

Fig. 4: (a) UV-Vis spectra of CM (10 μM) upon gradual addition of HSO_3^- (0 to 5 equivalents). (b) UV-Vis spectra of CM (10 μM) upon addition of 5 equivalents of stated analytes.

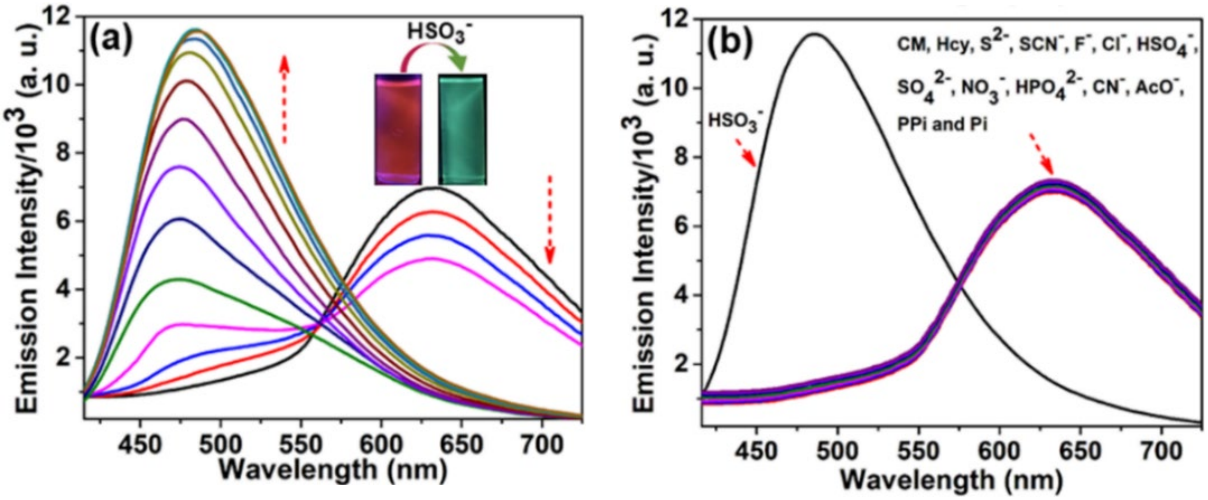

Fig. 5: (a) Change of emission spectra of **CM** (10 μM) upon gradual addition of HSO_3^- (0 to 5 equivalents). (b) Changes of emission spectra of **CM** (10 μM) upon addition of 5 equivalents of stated analytes. λ_{ex} = 410 nm.

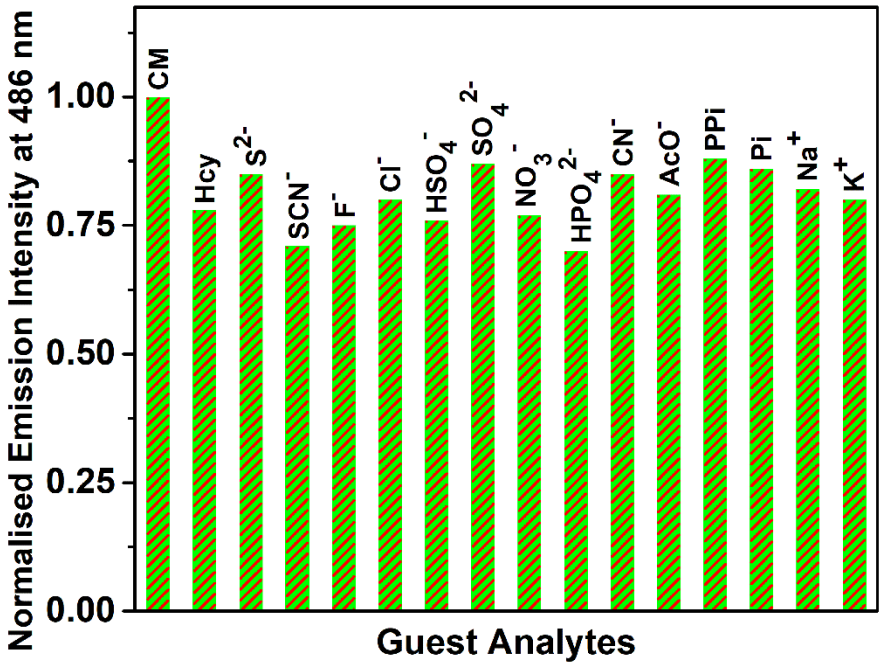

Fig. 6. A comparative study of normalised emission intensity after addition of different analytes (3 equivalents) in the solution of CM (10 μM) in presence of HSO_3^- (2 equivalents) λ_{ex} = 410 nm.

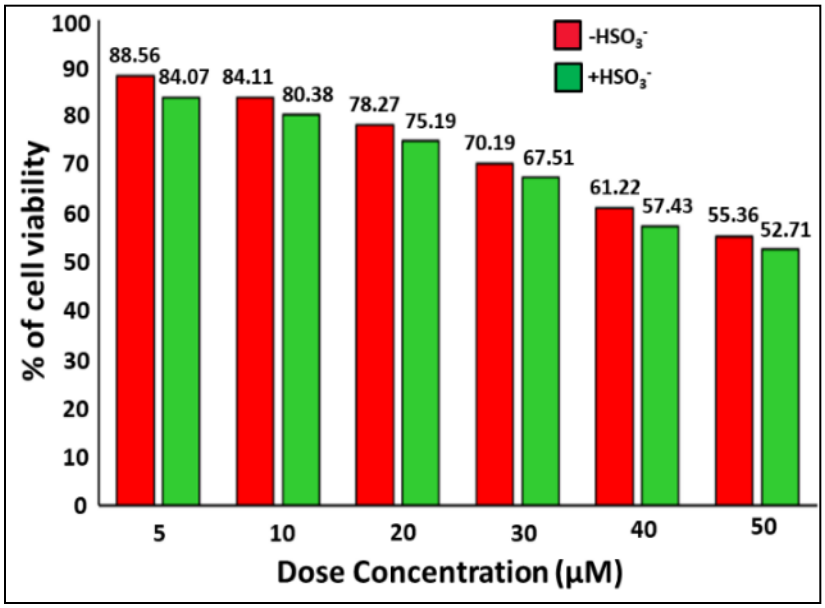

Fig. 7. Percentage of viable cells over CM concentration range (5-50 μM) presence and absence of HSO_3^-.

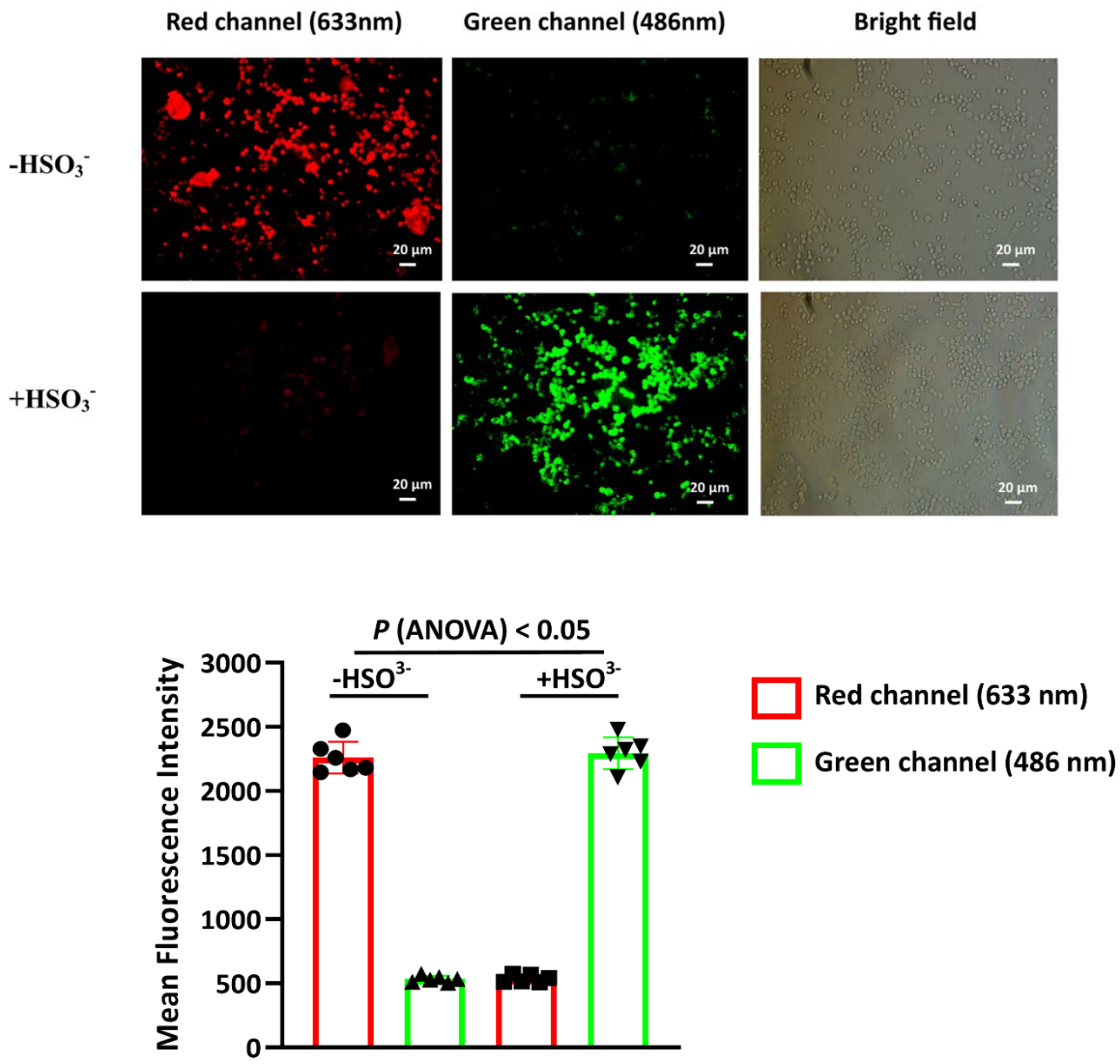

Fig. 8: A. Fluorescence images (40x) of human PBMCs treated with (upper) and without (lower) HSO_3^- (25 µM) along with 10 µM CM. Images were taken at red (emission at 633 nm) and green channel (emission at 486 nm) channel. λ_{ex}= 410 nm. CM (10 µM) could successfully detect HSO_3^- in cells and the fluorescence has shifted from red to green. Whereas without HSO_3^- no significant green signals were detected. Bright field images were given along with for each condition. B. The mean fluorescence intensities were measured in ImageJ, which shows a significant ($P < 0.05$) shifts from red (537 ± 29.8) to green (2295 ± 124.8) fluorescence when HSO_3^- was added. When there was no HSO_3^- present red fluorescence (2259.3 ± 124.1) was

significantly ($P < 0.05$) more visible than green (533.6 ± 25.2). The P values were calculated using one-way ANOVA followed by multiple comparison for differences between groups. Statistical calculations were carried out using GraphPad Prism 8.

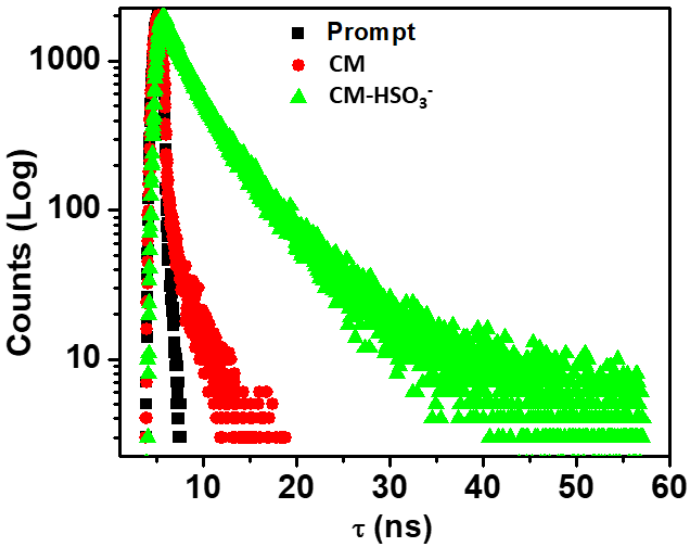

Fig. 9: Time-resolved fluorescence decay of **CM** (Red) and CM+HSO_3^- (Green).

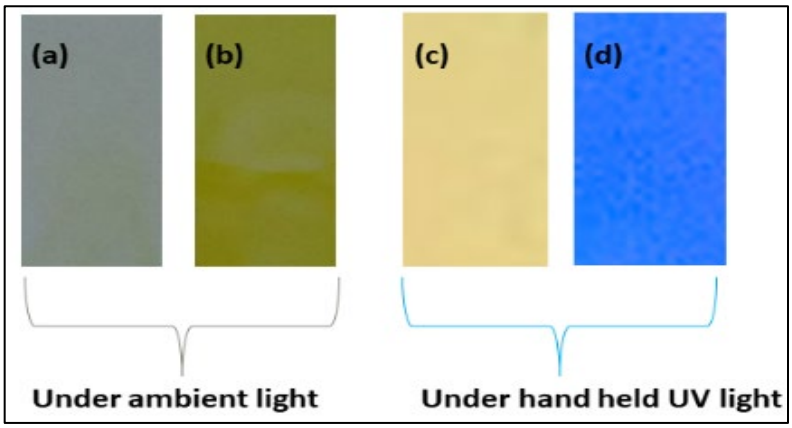

Fig. 10: Photographs of TLC plates soaked in the solution of **CM** before (a & c) and after addition of $NaHSO_3$ solution (b & d) (Left side under ambient light; Right side under hand held UV light).